JOURNAL OF GUIDANCE, CONTROL, AND DYNAMICS
Vol. 23, No. 5, September–October 2000

Minimum Power Optimum Control of Microsatellite Attitude Dynamics

Michele Grassi*
University of Naples "Federico II," 80125 Naples, Italy
and
Massimiliano Pastena†
Second University of Naples, 81031 Aversa, Italy

This paper deals with the attitude dynamics and control of a multimission microsatellite for remote sensing applications. The attitude control system consists of three small reaction wheels and three magnetic torquers. The paper presents a new control technique in which the required control torque is continuously redistributed between the reaction wheels and the magnetic torquers to minimize the electric power consumption in the attitude control. The required control torque is computed using proportional derivative control laws and the optimum control theory. Numerical results show that substantial power savings can be obtained while retaining attitude control accuracy adequate for remote sensing applications.

Introduction

MICROSATELLITES represent a flexible tool to carry out scientific and technological research in space. Nevertheless, obvious limitations in size, mass, onboard available power, and costs impose several constraints on the design of the microsatellite subsystems. The attitude control subsystem, as one of the more complex subsystems of a satellite, is particularly affected by these constraints, especially when the considered applications require stringent attitude control. Therefore, new solutions in terms of components and operating logic need to be investigated to reduce costs, volume, and power requirements.

Several authors have studied the attitude control of a microsatellite. The use of environmental torques, such as those caused by gravity, the Earth's magnetic field, and aerodynamic drag, to control the microsatellite attitude by means of passive and/or semipassive devices allows substantial mass and power savings. With regard to this, various solutions have been proposed based on the use of gravity gradient booms with eddy current dampers,[1] fluid ring dampers, or soft-magnetic damping rods[1,2] to damp the microsatellite residual attitude motion. Nevertheless, these solutions achieve a poor attitude control accuracy (5–10 deg). When a finer control is required, as in the case of remote sensing applications (0.1 deg), various configurations of low-mass, low-power momentum/reaction wheels have been proposed. In this case the use of magnetic torques for momentum dumping, as an alternative to more traditional gas jets,[3] reduces the control system complexity and mass. Because of its low mass and power consumption requirements, magnetic control is of particular interest for microsatellites: it is extensively adopted also for active attitude damping in gravity gradient stabilized satellites, initial despin, attitude acquisition, and precession control.[4,5]

This paper deals with the attitude control of the Italian Scientific Microsatellite for Advanced Research and Technology (SMART). The engineering model of the microsatellite has been designed and realized at the Universities of Naples. SMART is a multimission microsatellite for remote sensing applications in sun-synchronous orbits with altitudes ranging from 400 to 1000 km.[6] Figure 1 shows the microsatellite preliminary configuration, whereas Table 1 lists its main characteristics.

Received 9 April 1997; revision received 22 October 1998; accepted for publication 4 January 2000.

*Professor of Aerospace Systems, Dipartimento di Scienza e Ingegneria dello Spazio, p.le Tecchio 80.

†Ph.D. in Aerospace Engineering, Dipartimento di Ingegneria Aerospaziale, Real Casa dell'Annunziata, via Roma 29.

The microsatellite attitude control system consists of three small reaction wheels and three magnetic torquers (torquerods). The wheels, mounted with their axes aligned along the microsatellite geometrical axes, are used for three-axes attitude control during station keeping. The reaction wheel design has been performed using a technique that, for given wheel performance (in terms of maximum reaction torque and angular momentum capacity), minimizes mass and power consumption.[7] The wheel and control electronics are under development at the Second University of Naples. As far as the magnetic torquer design is concerned, it was preliminarily driven by the requirements for onboard wheel momentum unloading and initial attitude acquisition following the separation from the launcher. Nevertheless, the possibility of using the magnetic torquers for attitude control during station keeping can be also considered. In this case techniques must be studied to distribute the control action among dissimilar actuators.[8] In this paper a technique is proposed to distribute the torque required for attitude control between wheels and magnetic torquers, which minimizes the total power consumption. In particular, because the reaction wheel design has been already optimized with respect to mass and power consumption the proposed technique is used mainly to optimize the magnetic torquer design. To this end, the torque required for the attitude control is first determined using proportional-derivative (PD) control laws and optimal control theory. The control torque is then continuously redistributed between wheels and torquerods along the orbit so that the electric power consumption is minimized. The control technique is tested using a numerical code that simultaneously integrates the satellite orbital and attitude dynamics and control considering the main environmental perturbations. Finally, the effect of the proposed technique on attitude control accuracy is numerically evaluated.

Analytical Model

For the satellite attitude analysis three reference frames are introduced (Fig. 1): the orbiting reference frame (whose origin is at the satellite center of mass, the z_0 axis is aligned with the satellite position vector and directed downward, the x_0 axis is directed along the velocity vector, and the y_0 axis completes a right-handed reference frame); the attitude reference frame (ARF) (fixed to the satellite, with origin at the satellite center of mass and axes x, y, and z aligned along the axes of the orbiting reference frame at zero attitude angles); and the body reference frame (with origin at the satellite center of mass), whose axes 1, 2, and 3 coincide with the satellite inertia principal axes and are rotated by the angles γ_0, β_0, and α_0 (3-2-1 sequence) (Table 1) with respect to the ARF axes. The analytical model of the satellite attitude is based on the following assumptions: 1) satellite center of mass in Keplerian circular orbit, 2) gravitational potential linearized, and 3) small attitude angles in

Table 1 Simulation main parameters

Parameter	Value
Orbit	Circular, sun-synchronous (10p.m. ÷ 12p.m.)
Altitude range, km	From 400 to 1000
Mass, kg	50
Bus size, m	$0.35 \times 0.35 \times 0.60$ h
Satellite inertia tensor, kg m^2	$\begin{bmatrix} 73.1 & 4.21\cdot10^{-4} & -4.86\cdot10^{-2} \\ 4.21\cdot10^{-4} & 7.47 & -5.80\cdot10^{-3} \\ -4.86\cdot10^{-2} & -5.80\cdot10^{-3} & 4.50\cdot10^{-1} \end{bmatrix}$
Orientation of BRF with respect to ARF (3-2-1 sequence), deg	$\gamma_0 = -2.0\cdot10^{-1}$ $\beta_0 = 4.0\cdot10^{-1}$ $\alpha_0 = 5.0\cdot10^{-2}$
Control law gain matrix	$\begin{bmatrix} 3.66\cdot10^{-2} & 0 & -2.19\cdot10^{-3} & 7.31\cdot10^{-1} & 0 & -6.00\cdot10^{-2} \\ 0 & 3.74\cdot10^{-2} & 0 & 0 & 7.47\cdot10^{-1} & -6.72\cdot10^{-3} \\ 1.35\cdot10^{-4} & 0 & 2.25\cdot10^{-3} & 8.55\cdot10^{-4} & 1.35\cdot10^{-4} & 4.50\cdot10^{-1} \end{bmatrix}$
Closed-loop poles	Real part / Imaginary part $-9.95\cdot10^{-1}$ / 0 $-5.04\cdot10^{-3}$ / 0 $-5.01\cdot10^{-2}$ / $5.02\cdot10^{-2}$ $-5.00\cdot10^{-2}$ / $5.01\cdot10^{-2}$
Reaction wheel	
Total mass, kg	0.23
Diameter, m	0.10
Inertia moment, kg m^2	$1.60\cdot10^{-4}$
Motor torque constant, mNm/A	30.38
Motor winding resistance, Ohm	105
No-load current, mA	4
Wheel torque error, Nm[11]	1% of maximum torque
Magnetometer meas. error (Tesla)	$3\cdot10^{-7}$
Torquerod linearity error[11]	4%

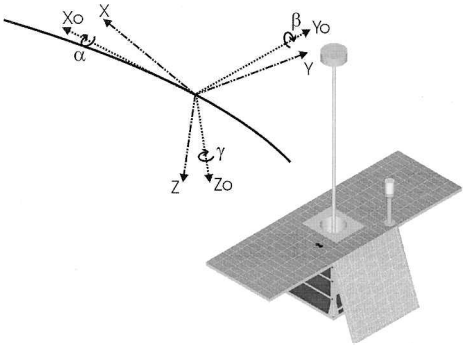

Fig. 1 SMART configuration and reference frames.

the presence of attitude control. The satellite attitude equations in matrix form in ARF are as follows:

$$\boldsymbol{I}_n\ddot{\boldsymbol{q}} + \boldsymbol{C}_s\dot{\boldsymbol{q}} + \boldsymbol{K}\boldsymbol{q} = \boldsymbol{Q}_f \tag{1}$$

where

$$\boldsymbol{q} = [\,\alpha \quad \beta \quad \gamma\,]^T, \qquad \boldsymbol{Q}_f = \left[\,4\omega_0^2 I_{yz} + M_{cx} + M_{ex} \quad -3\omega_0^2 I_{xy} + M_{cy} + M_{ey} \quad -\omega_0^2 I_{xy} + M_{cz} + M_{ez}\,\right]^T \tag{2}$$

and the T superscript indicates transposition.

The $\boldsymbol{I}_n$, $\boldsymbol{C}_s$, and $\boldsymbol{K}$ matrices in Eq. (1) have the following expressions:

$$\boldsymbol{I}_n = \begin{bmatrix} I_x & -I_{xy} & -I_{xz} \\ -I_{xy} & I_y & -I_{yz} \\ -I_{xz} & -I_{yz} & I_z \end{bmatrix} \tag{3a}$$

$$\boldsymbol{C}_s = \omega_0 \begin{bmatrix} 0 & 2I_{yz} & -(I_x + I_z - I_y) \\ -2I_{yz} & 0 & 2I_{xy} \\ (I_x + I_z - I_y) & -2I_{xy} & 0 \end{bmatrix} \tag{3b}$$

$$\boldsymbol{K} = \omega_0^2 \begin{bmatrix} 4(I_y - I_z) & 3I_{xy} & -I_{xz} \\ 4I_{xy} & 3(I_x - I_z) & I_{yz} \\ -4I_{xz} & -3I_{yz} & (I_y - I_x) \end{bmatrix} \tag{3c}$$

where ω_0 is the orbital angular velocity of the satellite center of mass, M_{ci} and M_{ei} are the ith components in ARF of the control and external disturbing torques, respectively, and I_x, I_y, I_z, I_{xy}, I_{xz}, I_{yz} are the satellite moments and products of inertia (Table 1).

In the state space Eq. (1) can be rewritten as follows:

$$\dot{\boldsymbol{x}} = \boldsymbol{A}\boldsymbol{x} + \boldsymbol{B}_s(\boldsymbol{M}_d + \boldsymbol{M}_c) \tag{4}$$

where $\boldsymbol{x}$, $\boldsymbol{M}_d$, and $\boldsymbol{M}_c$ are the system state vector, disturbance input vector, and control input vector, respectively:

$$\boldsymbol{x} = [\,\alpha \quad \beta \quad \gamma \quad \dot{\alpha} \quad \dot{\beta} \quad \dot{\gamma}\,]^T$$

$$\boldsymbol{M}_d = \left[\,4\omega_0^2 I_{yz} + M_{ex} \quad -3\omega_0^2 I_{xy} + M_{ey} \quad -\omega_0^2 I_{xy} + M_{ez}\,\right]^T$$

$$\boldsymbol{M}_c = [\,M_{cx} \quad M_{cy} \quad M_{cz}\,]^T \tag{5}$$

and the $\boldsymbol{A}$ and $\boldsymbol{B}_s$ matrices are given by the following expressions[9]:

$$\boldsymbol{A} = \begin{bmatrix} \boldsymbol{0} & \boldsymbol{I} \\ -\boldsymbol{I}_n^{-1}\boldsymbol{K} & -\boldsymbol{I}_n^{-1}\boldsymbol{C}_s \end{bmatrix}, \qquad \boldsymbol{B}_s = \begin{bmatrix} \boldsymbol{0} \\ \boldsymbol{I}_n^{-1} \end{bmatrix} \tag{6}$$

where $\boldsymbol{0}$ and $\boldsymbol{I}$ are the 3×3 null matrix and the 3×3 identity matrix, respectively.

Attitude Control

Three-axis attitude control during station keeping is performed simultaneously using three reaction wheels and three torquerods mounted with their axes aligned along the ARF axes. Therefore, the input control vector is obtained by the vector sum of the control torques given by torquerods ($\boldsymbol{M}_{ct}$) and reaction wheels ($\boldsymbol{M}_{cw} = -\dot{\boldsymbol{h}}_w$):

$$\boldsymbol{M}_c = \boldsymbol{M}_{cw} + \boldsymbol{M}_{ct} = -\dot{\boldsymbol{h}}_w + \boldsymbol{d} \times \boldsymbol{B} \tag{7}$$

where $\boldsymbol{h}_w$ is the wheel angular momentum vector, $\boldsymbol{d}$ is the magnetic dipole vector of the torquerods, and $\boldsymbol{B}$ is the Earth's magnetic induction vector. Because the use of orbit-rate coupled wheel commands

requires the continuous measurement of the orbit rate and causes resonance in the presence of low-frequency (of order ω_0) external disturbing torques, to simplify the control logic the gyroscopic coupling terms are not included in the wheel control torque vector in Eq. (7). Therefore, Eq. (4) can be rewritten as follows:

$$\dot{\boldsymbol{x}} = \boldsymbol{A}\boldsymbol{x} + \boldsymbol{B}_s(\boldsymbol{M}_c + \boldsymbol{M}_d + \boldsymbol{M}_g) \tag{8}$$

where $\boldsymbol{M}_g$ accounts for the gyroscopic coupling terms caused by the reaction wheels and is given by the following expression:

$$\boldsymbol{M}_g = -\boldsymbol{\omega} \times \boldsymbol{h}_w \tag{9}$$

where $\boldsymbol{\omega}$ is the inertial angular velocity vector.

Control Law

With respect to momentum wheels, reaction wheels are usually designed to independently control the satellite attitude around three orthogonal axes.[10] This requires reaction wheels with zero nominal angular momentum and low angular momentum capacity in order to reduce unwanted cross coupling during control. As a consequence, the $\boldsymbol{M}_g$ term is small and can be neglected in the closed-loop system design. This is confirmed by subsequent numerical simulations.

Using a PD control law, the control input vector can be expressed as follows:

$$\boldsymbol{M}_c = -\boldsymbol{G}\boldsymbol{x} \tag{10}$$

The 3×6 gain matrix $\boldsymbol{G}$ is evaluated with the optimal control theory minimizing the following performance index[11]:

$$V = \int_t^\infty \left[\boldsymbol{x}^T(\tau)\boldsymbol{Q}\boldsymbol{x}(\tau) + \boldsymbol{M}_c^T(\tau)\boldsymbol{R}\boldsymbol{M}_c(\tau)\right] \mathrm{d}\tau \tag{11}$$

The $\boldsymbol{Q}$ and $\boldsymbol{R}$ diagonal matrices are numerically evaluated, by trial and error, in order to have closed-loop system poles that realize a good tradeoff between control system performance (in terms of steady-state values and bandwidth) and control input magnitude.[11] Thus, Eq. (10) gives the control torque vector required to have the desired performance. The numerical values of the gain matrix and of the closed-loop poles are given in Table 1.

Control Torque Distribution

The distribution of the required control torque between the reaction wheels and the torquerods is performed so that the total electric power consumption is minimized. The control performance (in terms of bandwidth and steady-state values) is determined only by the selected gain matrix $\boldsymbol{G}$ [see Eq. (10)]. As a consequence, if the gyroscopic coupling terms and the actuator errors are neglected the required control torque and the attitude control performance are not affected by the torque distribution between wheels and torquerods. It is then possible to assume that the total electric power converted into mechanical power in the control is unaffected by the torque distribution. Therefore, the minimization process can be limited to the total electric power dissipated in the control, namely, the electric power converted into heat.

The torquerod magnetic dipole vector and the wheel reaction torque vector can be expressed, respectively, as follows[12]:

$$\boldsymbol{d} = (\mu_r n_s A_t)\boldsymbol{I}_t \tag{12a}$$

$$\dot{\boldsymbol{h}}_w = k_m(\boldsymbol{I}_w - \boldsymbol{I}_o) = k_m \boldsymbol{I}_{wa} \tag{12b}$$

where n_s is the number of torquerod windings, μ_r is the relative permeability of the torquerod core material, A_t is the area enclosed by a wire loop, $\boldsymbol{I}_t$ is the vector whose ARF components are the supply currents of the three torquerods, k_m is the torque constant of the dc motors driving the wheels, $\boldsymbol{I}_w$ and $\boldsymbol{I}_o$ are vectors whose ARF components are the supply and no-load currents of the three motors, respectively.

If reaction wheels and torquerods are simultaneously used for the attitude control, the total electric power dissipated in the control is given by the following expression:

$$P_{\mathrm{dtot}} = R_m\left[(I_{\mathrm{wax}})^2 + (I_{\mathrm{way}})^2 + (I_{\mathrm{waz}})^2\right] + R_t\left(I_{tx}^2 + I_{ty}^2 + I_{tz}^2\right) \tag{13}$$

where R_t and R_m are the resistances of the torquerod and motor windings, respectively. Using Eqs. (7) and (12), P_{dtot} can be expressed as a function of the torquerod magnetic dipole and control input vectors ARF components as follows:

$$P_{\mathrm{dtot}} = \left(R_m / k_m^2\right)\left[(M_{cx} - d_y B_z + d_z B_y)^2 + (M_{cy} - d_z B_x + d_x B_z)^2 + (M_{cz} - d_x B_y + d_y B_x)^2\right] + \left[R_t / (\mu_r n_s A_t)^2\right]\left(d_x^2 + d_y^2 + d_z^2\right) \tag{14}$$

where B_x, B_y, and B_z are the ARF components of the Earth's magnetic induction vector. Equation (14) shows that, for a given control input vector, a magnetic dipole vector can be found that minimizes the total electric power dissipated in the attitude control. This magnetic dipole vector is a function of the torquerod and wheel parameters and of the Earth's magnetic field vector, whose magnitude and direction vary along the orbit. The magnetic dipole vector that minimizes P_{dtot} is evaluated as follows:

$$\frac{\partial P_{\mathrm{dtot}}}{\partial d_x} = 0, \qquad \frac{\partial P_{\mathrm{dtot}}}{\partial d_y} = 0$$

$$\frac{\partial P_{\mathrm{dtot}}}{\partial d_z} = 0 \Rightarrow \boldsymbol{d} = \Delta^{-1}\frac{2R_m}{k_m^2}(\boldsymbol{B} \times \boldsymbol{M}_c) \tag{15}$$

where Δ is a time-varying coefficient matrix given by the following expression:

$$\Delta = \begin{bmatrix} \left[\frac{2R_t}{(\mu_r n_s A_t)^2} + \frac{2R_m}{k_m^2}\left(B_y^2 + B_z^2\right)\right] & -\left(\frac{2R_m B_y B_x}{k_m^2}\right) & -\left(\frac{2R_m B_x B_z}{k_m^2}\right) \\ -\left(\frac{2R_m B_y B_z}{k_m^2}\right) & \left[\frac{2R_t}{(\mu_r n_s A_t)^2} + \frac{2R_m}{k_m^2}\left(B_x^2 + B_z^2\right)\right] & -\left(\frac{2R_m B_z B_y}{k_m^2}\right) \\ -\left(\frac{2R_m B_x B_z}{k_m^2}\right) & -\left(\frac{2R_m B_z B_y}{k_m^2}\right) & \left[\frac{2R_t}{(\mu_r n_s A_t)^2} + \frac{2R_m}{k_m^2}\left(B_x^2 + B_y^2\right)\right] \end{bmatrix} \tag{16}$$

Using Eq. (15), it is possible to evaluate the magnetic control torque vector as follows:

$$\boldsymbol{M}_{\mathrm{ct}} = \boldsymbol{d} \times \boldsymbol{B} = \Delta^{-1}\left(2R_m / k_m^2\right)[(\boldsymbol{B} \times \boldsymbol{M}_c) \times \boldsymbol{B}] \tag{17}$$

As expected, the control torque percentage assigned to the torquerods is a function of the torquerod and wheel parameters and of the Earth's magnetic field because the magnetic control efficiency strongly depends on the variation of the field magnitude and direction along the orbit. As a consequence, for given wheel and torquerod parameters a continuous redistribution of the control torque is performed along the orbit. Therefore, the torquerod magnetic dipole vector and the wheel reaction torque are continuously recalculated using Eqs. (15) and (18).

The wheel reaction torque vector is evaluated, using Eq. (7), as the difference between the required control torque vector and the torquerod torque vector:

$$-\dot{\boldsymbol{h}}_w = \boldsymbol{M}_c - \boldsymbol{M}_{\mathrm{ct}} = \boldsymbol{M}_c - \Delta^{-1}\left(2R_m / k_m^2\right)[(\boldsymbol{B} \times \boldsymbol{M}_c) \times \boldsymbol{B}] \tag{18}$$

The simultaneous use of Eqs. (17) and (18) allows the required control torque in Eq. (10) to be always realized. In addition, Eqs. (17) and (18) show that, as a consequence of the torque distribution, the wheel control torque vector also depends on the torquerod parameters and on the Earth's magnetic field. In subsequent numerical analysis, the control technique performance, in terms of power saving and attitude control accuracy, is analyzed vs the parameter $R_t/(\mu_r n_s A_t)^2$ (torquerod design parameter), which, for given dc motor characteristic and Earth's magnetic field magnitude and direction, determines the required torque percentage assigned to the torquerod.

Attitude Control Error Budget

To evaluate the effect of the proposed control technique on the attitude control accuracy, the following error sources are considered in the evaluation of the control input vector uncertainty: 1) the uncertainty in the estimate of the motor torque constant σ_{k_m}; 2) the magnetometer measurement error σ_{B_i}; and 3) the uncertainty in the estimate of the torquerod scale factor ($scf = \mu_r n_s A_t$), σ_{scf}.

The torquerod scale factor error is evaluated from the torquerod linearity error[13] (Table 1). Because the SMART reaction wheels are under development,[7] the motor torque constant error is evaluated using Ref. 13 (Table 1).

Assuming uncorrelated parameters, the uncertainty in the evaluation of the torquerod dipole vector ARF components is computed as follows[14]:

$$\left[\sigma_{de}^2\right]_i = \left[\left(\frac{\partial \boldsymbol{d}}{\partial k_m}\right)_i\right]^2 \sigma_{k_m}^2 + \left[\left(\frac{\partial \boldsymbol{d}}{\partial scf}\right)_i\right]^2 \sigma_{\text{scf}}^2 + \left[\left(\frac{\partial \boldsymbol{d}}{\partial B_x}\right)_i\right]^2 \sigma_{B_x}^2 + \left[\left(\frac{\partial \boldsymbol{d}}{\partial B_y}\right)_i\right]^2 \sigma_{B_y}^2 + \left[\left(\frac{\partial \boldsymbol{d}}{\partial B_z}\right)_i\right]^2 \sigma_{B_z}^2 \tag{19}$$

where the subscript i indicates ARF ith component and

$$\frac{\partial \boldsymbol{d}}{\partial k_m} = \left(\frac{2R_m}{k_m^2}\right)\left[-\left(\frac{2}{k_m}\right)\Delta^{-1} + \left(\frac{\partial \Delta^{-1}}{\partial k_m}\right)\right](\boldsymbol{B} \times \boldsymbol{M}_c)$$

$$\frac{\partial \boldsymbol{d}}{\partial scf} = \left(\frac{2R_m}{k_m^2}\right)\left(\frac{\partial \Delta^{-1}}{\partial scf}\right)(\boldsymbol{B} \times \boldsymbol{M}_c)$$

$$\frac{\partial \boldsymbol{d}}{\partial B_i} = \left(\frac{2R_m}{k_m^2}\right)\left[\left(\frac{\partial \Delta^{-1}}{\partial B_i}\right)(\boldsymbol{B} \times \boldsymbol{M}_c) + \Delta^{-1}\frac{\partial(\boldsymbol{B} \times \boldsymbol{M}_c)}{\partial B_i}\right] \tag{20}$$

The uncertainty in the evaluation of the wheel torque vector ARF components is computed using Eq. (7) as follows:

$$\left[\sigma_{h_{we}}^2\right]_i = \left[\frac{\partial(\boldsymbol{d} \times \boldsymbol{B})_i}{\partial d_x}\right]^2 \left[\sigma_{de}^2\right]_x + \left[\frac{\partial(\boldsymbol{d} \times \boldsymbol{B})_i}{\partial d_y}\right]^2 \left[\sigma_{de}^2\right]_y + \left[\frac{\partial(\boldsymbol{d} \times \boldsymbol{B})_i}{\partial d_z}\right]^2 \left[\sigma_{de}^2\right]_z + \left[\frac{\partial(\boldsymbol{d} \times \boldsymbol{B})_i}{\partial B_x}\right]^2 \sigma_{B_x}^2 + \left[\frac{\partial(\boldsymbol{d} \times \boldsymbol{B})_i}{\partial B_y}\right]^2 \sigma_{B_y}^2 + \left[\frac{\partial(\boldsymbol{d} \times \boldsymbol{B})_i}{\partial B_z}\right]^2 \sigma_{B_z}^2 \tag{21}$$

Thus the total uncertainty in the torquerod magnetic dipole and in the wheel control torque can be evaluated considering the contributions given by Eqs. (19) and (21), the torquerod linearity error and the wheel torque error,[13] respectively, as follows:

$$\left[\sigma_d^2\right]_i = \left[\sigma_{de}^2\right]_i + \left[\left(\frac{\partial \boldsymbol{d}}{\partial scf}\right)_i\right]^2 \sigma_{\text{scf}}^2$$

$$\left[\sigma_{h_w}^2\right]_i = \left[\sigma_{h_{we}}^2\right]_i + \left[\sigma_{h_w\ \text{wheel}}^2\right]_i \tag{22}$$

The attitude covariance matrix is finally evaluated, by integration of the Riccati equation,[15] considering only the errors in the control input vector from the proposed technique:

$$\dot{\boldsymbol{P}} = \boldsymbol{A}_c\boldsymbol{P} + \boldsymbol{P}^T\boldsymbol{A}_c + \boldsymbol{B}_s\boldsymbol{Q}_{M_c}\boldsymbol{B}_s^T \tag{23}$$

where $\boldsymbol{A}_c = \boldsymbol{A} - \boldsymbol{B}_s\boldsymbol{G}$ and $\boldsymbol{Q}_{M_c}$ is the control input covariance matrix.

Numerical Results

Numerical simulations have been run to test the proposed control technique. To this end a numerical code has been used that simultaneously integrates the satellite orbital dynamics, considering the main environmental perturbations (the aerodynamic drag, the force of gravity, including the second zonal harmonic of the gravity field), and the satellite attitude dynamics and control.[16] The satellite attitude is simulated using the kinematics and Euler's differential equations, in which the unknown quantities are the Euler's angles of ARF with respect to a right-handed inertial reference frame (whose origin is at the Earth's center, the X axis is directed along the first point of Aries, and the X–Y plane coincides with the equatorial plane) and the ARF components of the inertial angular velocity vector, respectively.[16] The torques are evaluated considering the aerodynamic drag, the gravity gradient, and the attitude control. The total aerodynamic drag is computed by adding the contribution of each geometrical element, which, collectively, approximate the satellite shape, and neglecting the satellite attitude effect. The torquerod control torque is computed using the IGRF'85 model to simulate the Earth's magnetic field.[12,17]

Table 1 shows the numerical values of some parameters used in the numerical simulation, including the control law gain matrix and the microsatellite inertia tensor.

Figure 2 shows the microsatellite attitude angles in the case of minimum power optimal control. Initial values of 3, 3, and 5 deg have been assumed, respectively, for the roll, pitch, and yaw angles to model the end of the attitude acquisition phase, in which only a three-axis magnetometer and the three torquerods are used for attitude measurement and control, respectively.[17] It is possible to see that the attitude angles attain their steady-state values in about 1020 s. Table 2 lists the steady-state maximum values of the attitude angles and rates. The results are for a torquerod design parameter $R_t/scf^2 = 9.3 \cdot 10^{-3}$ Ohm/m^4, which has been preliminary considered for SMART microsatellite.

Figure 3 shows the wheel angular momentum components in the initial phase of the attitude control and during about 10 orbits. Because of the aerodynamic torque and because the satellite

Table 2 Attitude angle and rate steady-state maximum values

Axis	Angle, deg	Rate, deg/s
Roll	$4.7 \cdot 10^{-4}$	$7.0 \cdot 10^{-7}$
Pitch	$3.2 \cdot 10^{-3}$	$3.7 \cdot 10^{-7}$
Yaw	$1.8 \cdot 10^{-3}$	$8.0 \cdot 10^{-6}$

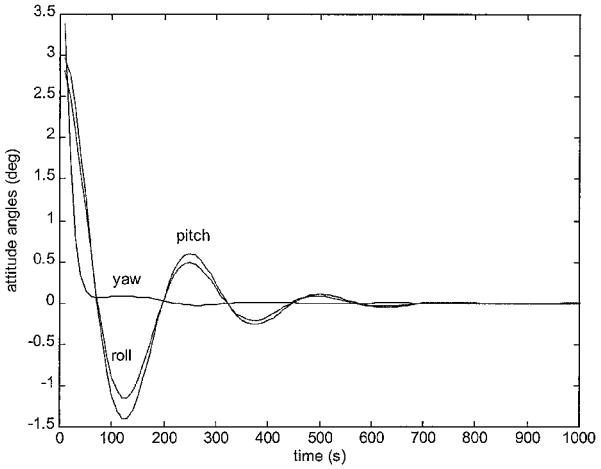

Fig. 2 Controlled attitude angles.

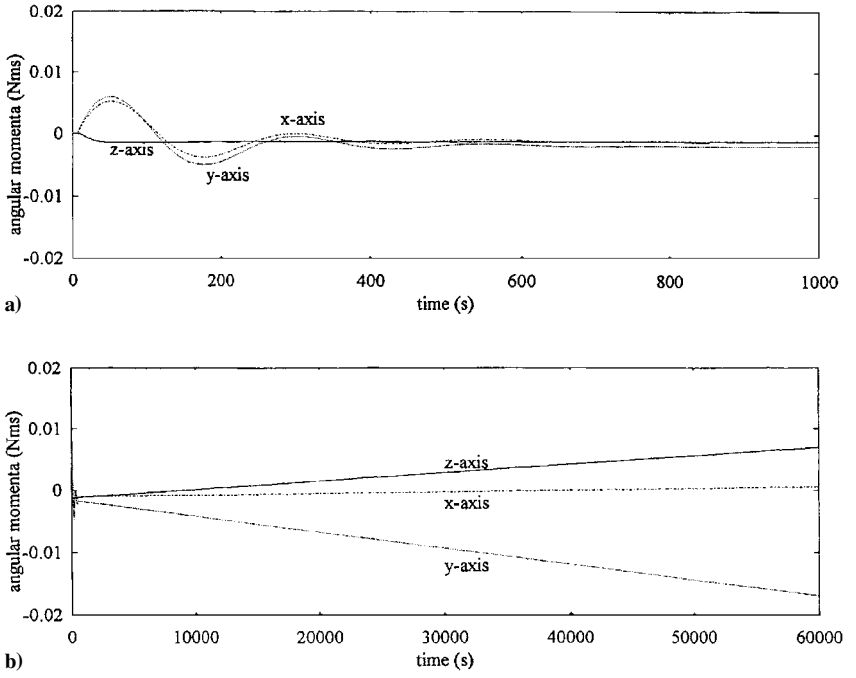

Fig. 3 Reaction wheel angular momentum components.

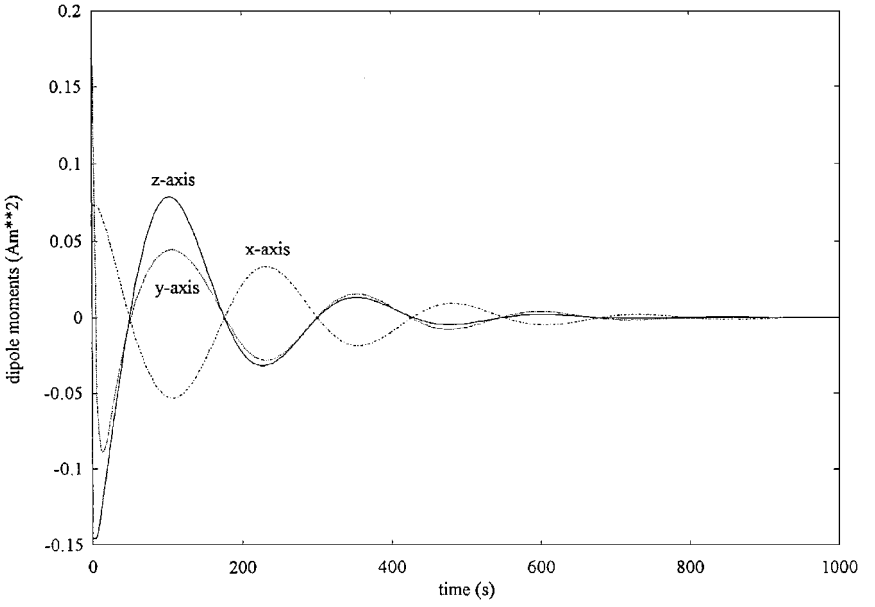

Fig. 4 Torquerod magnetic dipoles.

geometrical axes are rotated by small angles with respect to the inertia principal axes, the angular momenta exhibit a sinusoidal behavior around slowly increasing mean values. Nevertheless, according to the analytical model assumption the angular momenta attain small values. Figure 4 shows the torquerod magnetic dipole vector ARF components.

An index of the effectiveness of the proposed technique is the power saving with respect to the case of optimal control with reaction wheels only. The power saving is evaluated by averaging over an orbit the difference between the electric power dissipated in the case of control with reaction wheels only and the electric power dissipated in the case of minimum power optimal control. This difference is plotted in Fig. 5 vs the torquerod design parameter, as a percentage of the electric power dissipated in the case of control with wheels only. It can be seen that a substantial power saving can be obtained by reducing the torquerod design parameter. In fact, for given Earth's magnetic field magnitude and direction, as the torquerod parameter reduces, the torquerod efficiency increases, and, as a consequence, a greater portion of the required control torque is transferred from the wheels to the torquerods.

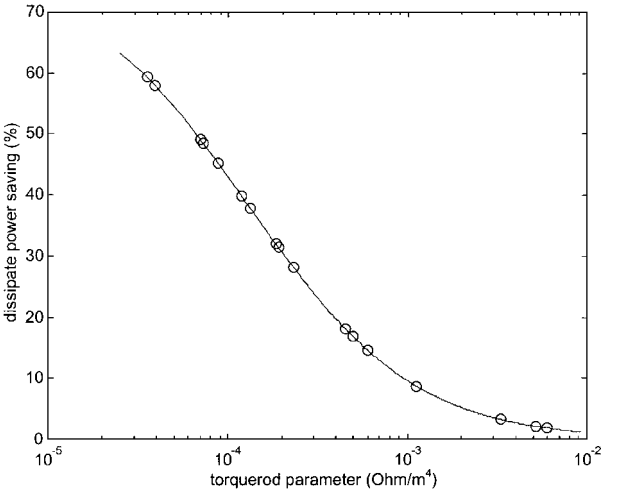

Fig. 5 Power saving percentage vs the torquerod design parameter.

The torquerod parameter preliminary considered for SMART allows a negligible power saving (about 1%). Therefore, to save more power, a smaller value of the parameter should be considered for the torquerod design. Because in the proposed control technique the required control torque is always realized, the use of a different torquerod design parameter produces only a variation in the gyroscopic coupling terms from the wheels. Nevertheless, because the gyroscopic coupling terms are small with respect to the reaction torques, the variation in the amplitudes of the controlled attitude angles can be neglected. This is confirmed by the analysis of Fig. 6, which shows the differences between the attitude angle steady-state values, caused only by the torque distribution, for two extreme cases: control with reaction wheels only and minimum power optimum control with $R_t/scf^2 = 2.5 \times 10^{-5}$ Ohm/m^4.

For values of the torquerod parameter lower than 0.0004 (Ohm/m^4), substantial power savings could be realized by slightly changing the torquerod design parameter. The circles in Fig. 5 mark on the diagram the performance of space qualified off-the-shelf torquerods.[13]

Figures 7 and 8 diagram the maximum values of the uncertainties in the required control torque ARF components and in the controlled attitude angles vs the torquerod design parameter, respectively. As R_t/scf^2 decreases, which means that a greater portion of the required control torque is being transferred to the torquerods, the attitude control accuracy reduces. On the other hand, as the torquerod design parameter increases the attitude control accuracy tends to the value in the case of optimal control with reaction wheels only.

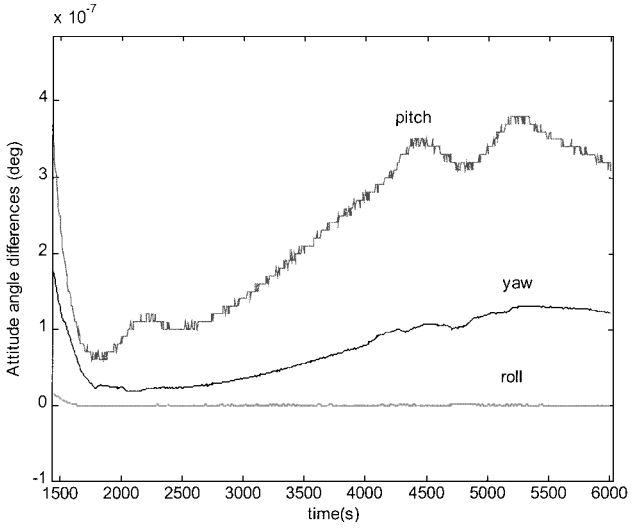

Fig. 6 Attitude angle differences.

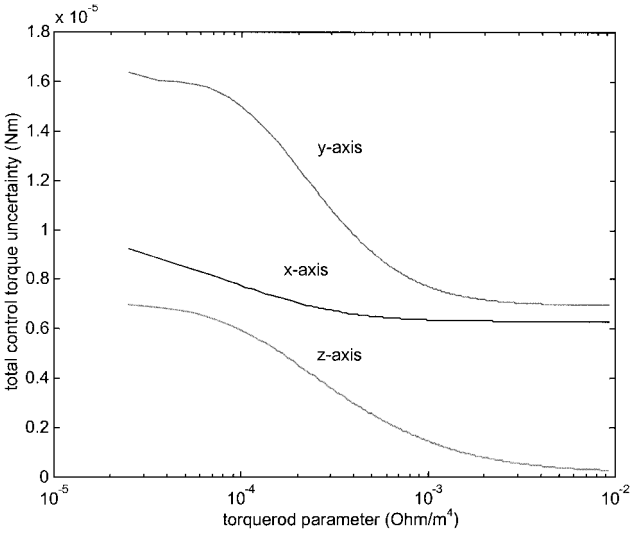

Fig. 7 Control torque uncertainty vs the torquerod design parameter.

Table 3 Attitude control accuracy

Axis	Attitude control accuracy, deg: Reaction wheels	Attitude control accuracy, deg: Reaction wheels and torquerods
Roll	7.9×10^{-4}	7.9×10^{-4}
Pitch	8.6×10^{-4}	1.2×10^{-3}
Yaw	9.0×10^{-4}	1.6×10^{-2}

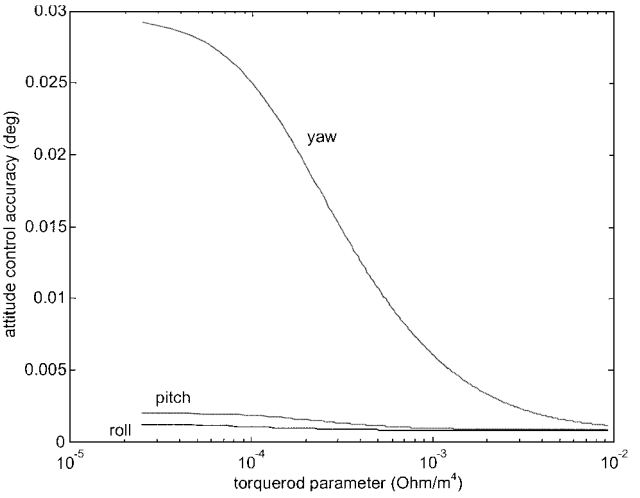

Fig. 8 Attitude control accuracy vs the torquerod design parameter.

Table 3 compares the attitude control accuracy in the two cases of optimal control with reactions wheels only and minimum power optimal control for a 40% power saving. Thanks to the selected gain matrix, the roll and pitch control accuracy are almost unaffected by the torque distribution. On the contrary, the yaw angle control accuracy reduces attaining the value of 0.016 deg, which is, however, adequate for remote sensing applications. Finally, the yaw angle control accuracy could be improved, at the cost of higher power consumption, simply increasing the corresponding gains in the $\boldsymbol{G}$ matrix.

Conclusions

This paper analyzed the attitude dynamics and control for a remote sensing microsatellite whose control system consists of three small reaction wheels and three torquerods. In particular, a new technique has been proposed, based on the simultaneous use of reaction wheels and torquerods, to have the required control torque with a minimum power consumption.

The paper presents the analytical model of the proposed technique and demonstrates its effectiveness by numerical simulations. In particular, the numerical analysis shows the following:

1) Wheels and torquerods can be simultaneously used to realize a required control torque with minimum power consumption.

2) The control torque distribution between torquerods and wheels is governed by the torquerod control efficiency, which strongly depends on the Earth's magnetic field variation along the orbit and on the torquerod design parameter R_t/scf^2 (where R_t is the torquerod winding resistance and scf is the ratio of the torquerod magnetic dipole to the torquerod supply current).

3) When more efficient torquerods are used, the control torque portion transferred to the torquerods increases so that the total power consumption is minimized.

4) The use of torquerods with low values of the design parameter allows substantial power savings with respect to the case of optimal control with reaction wheels only.

5) As the required torque percentage assigned to the torquerods increases, the attitude control accuracy reduces. Nevertheless, substantial power savings can be realized while retaining an attitude control accuracy adequate for remote sensing applications (0.016 deg for a 40% power saving).

6) The attitude control accuracy could be improved by slightly increasing the numerical values of the control gains at the cost of higher power consumption.

7) The proposed control technique could be used in addition to wheel momentum unloading and attitude acquisition considerations to design the satellite torquerods.

Finally, the proposed technique does not increase the attitude control system complexity and mass because the torquerods are also used for initial attitude acquisition and wheel momentum unloading.

Acknowledgments

The work in the paper was carried out with the financial contribution of the Italian Space Agency and the Ministry for Technology and Scientific Research.

References

[1]Ovchinnikov, M., Yu., "Simple Methods of Attitude Control for Small Satellites," International Academy of Astronautics, Paper 95-IAA.11.2.08, Oct. 1995.

[2]Siahpush, A., and Sexton, A., "A Study for Semi-Passive Gravity Gradient Stabilization of Small Satellites," *Proceedings of the 1st Utah State University Conference on Small Satellites*, Center for Space Engineering, Logan, UT, 1987.

[3]Siahpush, A., and Gleave, J., "A Brief Survey of Attitude Control Systems Utilizing Momentum Wheel Concepts for Small Satellites," *Proceedings of the 2nd Annual AIAA/Utah State University Conference on Small Satellites*, Center for Space Engineering, Logan, UT, 1988.

[4]Stickler, A. C., and Alfriend, K. T., "Elementary Magnetic Attitude Control System," *Journal of Spacecraft and Rockets*, Vol. 13, No. 5, 1976, pp. 282–287.

[5]Alfriend, K. T., "Magnetic Attitude Control System for Dual-Spin Satellites," *AIAA Journal*, Vol. 13, No. 6, 1975, pp. 817–822.

[6]Grassi, M., and Pastena, M., "Design of a Multi-Mission Micro-Satellite," *Space Technology*, Vol. 16, No. 4, 1996, pp. 197–213.

[7]Pastena, M., and Grassi, M., "Design and Test of a Small Reaction Wheels for a Multi-Mission Microsatellite," *Proceedings of the 14th Conference of the Italian Association of Aeronautics and Astronautics (AIDAA)*, Vol. 2, AIDAA, Naples, Italy, 1997, pp. 635–644.

[8]Queen, E. M., and Silverberg, L., "Optimal Control of a Rigid Body with Dissimilar Actuators," *Journal of Guidance, Control, and Dynamics*, Vol. 19, No. 3, 1996, pp. 738–740.

[9]Meirovitch, L., *Introduction to Dynamics and Control*, Wiley, New York, 1985, pp. 269–280.

[10]Agrawal, B. N., *Design of Geosynchronous Spacecraft*, Prentice–Hall, Upper Saddle River, NJ, 1986, pp. 149, 150.

[11]Friedland, B., *Control System Design: An Introduction to State-Space Methods*, McGraw–Hill, New York, 1986, pp. 222–246.

[12]Wertz, J. R. (ed.), *Spacecraft Attitude Determination and Control*, D. Reidel, Boston, 1978, pp. 204, 205.

[13]Ithaco Catalogue, "Torquerod Design Specification," Ithaco, 735 West Clinton Street, Box 6437, Ithaca, NY 14851-6437 USA, 1996.

[14]Bevington, F. R., *Data Reduction and Error Analysis for the Physical Sciences*, McGraw–Hill, New York, 1969, pp. 56–65.

[15]Gelb, A., (ed.), *Applied Optimal Estimation*, Massachusetts Inst. of Technology Press, Cambridge, MA, 1989, pp. 75–78.

[16]Moccia, A., Vetrella, S., and Grassi, M., "Attitude Dynamics and Control of a Vertical Interferometric Radar Tethered Altimeter," *Journal of Guidance, Control, and Dynamics*, Vol. 16, No. 2, 1993, pp. 264–269.

[17]Grassi, M., "Performance Evaluation of the UNISAT Attitude Control System," *Journal of the Astronautical Sciences*, Vol. 45, No. 1, 1997, pp. 57–71.